Multinuclear Magnetic Resonance Study of the Dileadtrichalcogenide Anions $Pb_2S_nCh_{3-n}^{2-}$ (Ch = Se or Te), Pb_2SSeTe^{2-}, and $M_2Se_3^{2-}$ (M = Sn and/or Pb) and the Crystal Structures of $(2,2,2\text{-crypt-}K^+)_2Sn_2Te_3^{2-}$ and $(2,2,2\text{-crypt-}K^+)_2Sn_2Se_3^{2-}$

Már Björgvinsson,[1] Hélène P. A. Mercier, Kenneth M. Mitchell, Gary J. Schrobilgen,* and Geertje Strohe

Department of Chemistry, McMaster University, Hamilton, Ontario L8S 4M1, Canada

Received August 25, 1992®

The new series of dileadtrichalcogenide anions $Pb_2S_nSe_{3-n}^{2-}$ and $Pb_2S_nTe_{3-n}^{2-}$ (n = 0–3) and Pb_2SSeTe^{2-} have been obtained by extraction of the appropriate quaternary or quinternary alloys of the type $KPb_xS_yCh_z$ (Ch = Se, Te, or Se/Te) in ethylenediamine (en) and characterized in en solution by ^{77}Se, ^{125}Te, and ^{207}Pb NMR spectroscopy. The NMR findings indicate that the solution structures of the anions are based on a trigonal bipyramid having axial lead atoms bonded to three chalcogen atoms in the equatorial plane. Direct and pairwise additivity trends among the $Pb_2S_nCh_{3-n}^{2-}$ (Ch = Se or Te) series show that $^1J(^{207}Pb-^{77}Se)$, $\delta(^{207}Pb)$, $\delta(^{77}Se)$, and $\delta(^{125}Te)$ decrease upon chalcogen atom substitution as follows: S → Te > Se → Te ≫ S → Se. The isostructural $Sn_2Se_3^{2-}$ and $SnPbSe_3^{2-}$ anions have also been prepared in en by reaction of K_2Se with SnSe and SnSe/PbSe mixtures, respectively, and represent the first examples of Sn(II) chalcogenide anions. Both anions were characterized in en solution by ^{77}Se, ^{117}Sn, ^{119}Sn, and ^{207}Pb NMR spectroscopy. The two-bond Sn(II)–Sn(II) and Sn(II)–Pb(II) coupling constants, $^2J(^{117}Sn-^{119}Sn)$ and $^2J(^{119}Sn-^{207}Pb)$, have been observed for the first time and represent unusually large values [i.e., $^2J(^{119}Sn-^{117}Sn)$ = 1514 Hz and $^2J(^{119}Sn-^{207}Pb)$ = 1145 Hz]. After removal of the nuclear dependence to give reduced coupling constants, $^1K_{M-Ch}$, and after allowances for relativistic effects, which are significant in the heavy-element spin–spin couplings being considered, the magnitudes of the relativistically corrected reduced couplings, $(^1K_{M-Ch})_{RC}$, of the tin, lead, and tin/lead trigonal bipyramidal cage anions are shown to be consistent with predominantly p-bonded cages. The syntheses and crystal structures are reported for two salts in which the $Sn_2Te_3^{2-}$ and $Sn_2Se_3^{2-}$ anions have been stabilized as a result of complexation of the potassium cations by 4,7,13,16,21,24-hexaoxa-1,-10-diazabicyclo[8.8.8]hexacosane (2,2,2-crypt). The crystal structure of $(2,2,2\text{-crypt-}K^+)_2Sn_2Te_3^{2-}$ was determined at −100 and 24 °C; it crystallizes in the trigonal system $P\bar{3}c1$, with two molecules in a unit cell of dimensions a = 11.703(4) [11.817(9)] Å and c = 21.945(6) [22.01(2)] Å at −100 °C [24 °C] with R = 0.0628 [0.102] for 757 [305] observed ($I > 2[2]\sigma(I)$) reflections. The compound $(2,2,2\text{-crypt-}K^+)_2Sn_2Se_3^{2-}$ crystallizes in the monoclinic system, space group $P2_1/n$, with four molecules in a unit cell of dimensions a = 10.342(3) Å, b = 46.976(6) Å, c = 11.402(4) Å, and β = 90.15(3)° at 24 °C with R = 0.089 for 3016 observed ($I > 2\sigma(I)$) reflections. In addition to 2,2,2-crypt-K^+ cations, the compounds contain the trigonal-bipyramidal homopolyatomic anions $Sn_2Te_3^{2-}$ and $Sn_2Se_3^{2-}$ having approximate D_{3h} point symmetry. In $Sn_2Te_3^{2-}$, the Sn–Te distances are 2.887(4) [2.887(8)] Å with Sn–Te–Sn angles of 68.7(1) [69.4(3)]° and Te–Sn–Te angles of 90.9(1) [90.8(2)]° and an axial Sn···Sn distance of 3.270(6) [3.287(17)] Å. In $Sn_2Se_3^{2-}$, the Sn–Se distances are 2.637(3)–2.677(3) Å with Sn–Se–Sn angles of 70.9(1)–71.1(1)° and Se–Sn–Se angles of 87.9(1)–92.1(1)° and an axial Sn···Sn distance of 3.090(3) Å. In both structures, the distance between the two axial tin atoms is substantially less than the accepted van der Waals contact.

Introduction

The series of dileadtrichalcogenide anions $Pb_2Se_nTe_{3-n}^{2-}$ (n = 0–3) were previously prepared and characterized in our laboratory.[2] Multinuclear magnetic resonance studies of the anions showed that their structures were based on a trigonal bipyramid with the lead atoms in the axial positions and the chalcogen atoms (Ch) in the equatorial plane (structure I). These findings were

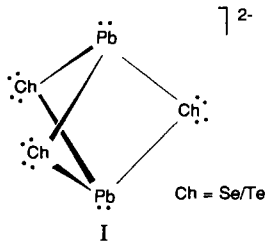

I

verified by the crystal structures of $(2,2,2\text{-crypt-}K^+)_2(Pb_2Se_3^{2-})$[2] and $(2,2,2\text{-crypt-}K^+)_2(Pb_2Te_3^{2-})$,[3] which showed the presence of flattened trigonal bipyramidal anions where the chalcogen atoms could be looked upon as having closest packing in the equatorial plane and bonded to the axial lead(II) atoms. As a consequence of the flattened nature of the trigonal bipyramids, Pb···Pb contacts that were significantly less than the van der Waals distance (4.0 Å)[4] were observed for the $Pb_2Se_3^{2-}$ [3.184(3) Å] and $Pb_2Te_3^{2-}$ [3.247(2) Å] anions. In light of these results, it was of interest to determine if a new series of dileadtrichalcogenide cage anions could be prepared by replacing one or more selenium and/or tellurium atoms with sulfur atoms. In addition, substitution of one or both axial lead atoms by tin atoms would give better insight into the nature of the short M···M distances in these flattened trigonal bipyramidal cages. The $Sn_2Ch_3^{2-}$ anions would represent the first examples of tinchalcogenide anions with tin in its +2 oxidation state.

Multinuclear magnetic resonance spectroscopy of the spin $^1/_2$ nuclei ^{77}Se, ^{117}Sn, ^{119}Sn, ^{125}Te, and ^{207}Pb is particularly well suited for their solution characterization, owing to the likely formation of mixtures of anions in the alloy extracts.[2,5] In addition to representative structural characterization in solution, atom

* Abstract published in *Advance ACS Abstracts*, October 1, 1993.

(1) Present address: Science Institute, University of Iceland, Dunhaga 3, 107 Reykjavík, Iceland.

(2) Björgvinsson, M.; Sawyer, J. F.; Schrobilgen, G. J. *Inorg. Chem.* **1987**, *26*, 741.

(3) Björgvinsson, M.; Sawyer, J. F.; Schrobilgen, G. J. *Inorg. Chem.* **1991**, *30*, 2231.

(4) Bondi, A. J. *Phys. Chem.* **1964**, *68*, 441.

0020-1669/93/1332-6046$04.00/0

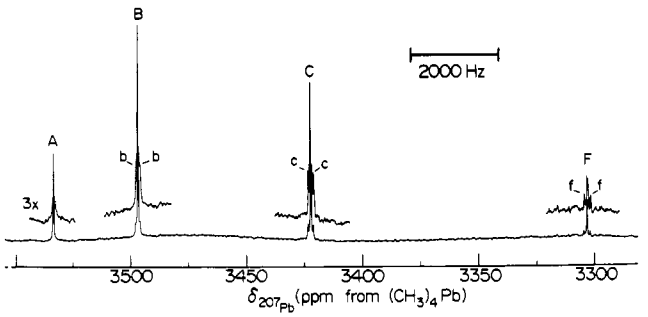

Figure 1. ^{207}Pb NMR spectrum (52.329 MHz) of the $Pb_2S_nSe_{3-n}^{2-}$ (n = 0–3) anion series recorded in en solvent at 24 °C: (A) $Pb_2S_3^{2-}$; (B) $Pb_2S_2Se^{2-}$; (C) $Pb_2SSe_2^{2-}$; (F) $Pb_2Se_3^{2-}$. Peaks labeled b, c, and f denote ^{77}Se satellites.

substitution effects on the chemical shifts and spin–spin coupling constants of the trigonal bipyramidal anions are also of interest. The replacement of one or both lead atoms with tin atoms is of particular interest as it provides an opportunity to observe the spin–spin coupling constants between the axial metal atoms.

Results and Discussion

Structural Characterization by Nuclear Magnetic Resonance Spectroscopy. The $Pb_2Ch_3^{2-}$ (Ch = S/Se, S/Te, and S/Se/Te) Anions. The experimental approach involved the syntheses of the materials $KPb_{0.40}S_{0.96}$, $KPb_{0.46}Se_{0.32}S_{0.63}$, $KPb_{0.45}Se_{0.63}S_{0.32}$, $KPb_{0.35}Te_{0.35}S_{0.64}$, $KPb_{0.50}Te_{0.70}S_{0.32}$, and $KPb_{0.35}Te_{0.35}Se_{0.32}S_{0.33}$ followed by extraction with ethylenediamine (en) in the presence of a slight excess of 2,2,2-crypt with respect to the K^+ ion. The resulting solutions were isolated from alloy residues, and the anions were identified in solution by direct NMR observation of the appropriate spin $^1/_2$ nuclei ^{77}Se, ^{125}Te, and ^{207}Pb at their natural abundance levels.

The new anion series, $Pb_2S_nSe_{3-n}^{2-}$ (Figure 1) and $Pb_2S_nTe_{3-n}^{2-}$ (Figure 2) (n = 0–3), were identified in solution from the number of observed environments, satellite doublet spacings [$^1J(^{77}Se$–$^{207}Pb)$ and $^1J(^{125}Te$–$^{207}Pb)$], and satellite peak/central peak area or height ratios in a manner analogous to that used for the previously studied $Pb_2Se_nTe_{3-n}^{2-}$ series.[2] The quaternary anion, Pb_2SSeTe^{2-}, was identified in a concentrated en solution after lengthy extraction of $Pb_{0.35}Te_{0.35}Se_{0.32}S_{0.33}$ along with the anion series $Pb_2S_nSe_{3-n}^{2-}$, $PbS_nTe_{3-n}^{2-}$, and $Pb_2Se_nTe_{3-n}^{2-}$ (Figure 2). The chemical shifts and spin–spin coupling constants for the new dileadtrichalcogenide anions are summarized in Table I.

In contrast to the spectra of the $Pb_2Se_nTe_{3-n}^{2-}$ (n = 0–3) series of anions,[2] no ^{77}Se NMR peak arising from the Se^{2-} anion was observed in the dileadtrichalcogenide anion solutions reported here, suggesting that the S^{2-} anion may be present instead. Unfortunately, this possibility could not be tested as it was not possible to observe the spherical S^{2-} anion in en solutions of $(2,2,2\text{-crypt-}K^+)_2S^{2-}$ by ^{33}S NMR spectroscopy. Failure to observe the ^{33}S resonance was presumed to be due to efficient quadrupolar relaxation of the ^{33}S nucleus resulting from fluctuating electric field gradients induced by en solvation.

The $M_2Se_3^{2-}$ (M = Sn and/or Pb) Anions. From previous studies in our laboratory it was apparent that only tin(IV) chalcogenide anions were formed in solution when alkali metal tin chalcogen alloys were extracted in en or liquid ammonia.[5,6] Consequently, in order to prepare the $Sn_2Se_3^{2-}$ anion, a mixture of K_2Se and SnSe in the ratio 1:2 was allowed to react directly in en in the presence of 2,2,2-crypt (eq 1). It was evident from the ^{77}Se NMR spectrum of the resulting yellow solution that unreacted Se^{2-} anion was the major species in solution (strong

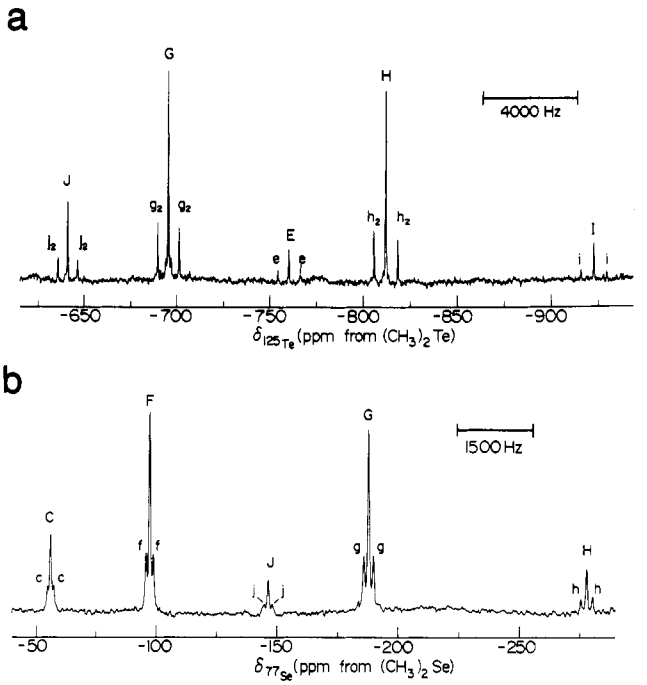

Figure 2. (a) ^{125}Te NMR spectrum (78.917 MHz) and (b) ^{77}Se NMR spectrum (47.704 MHz) of the $Pb_2Ch_3^{2-}$ (Ch = S/Se/Te) anions. Both spectra were recorded in en solvent at 24 °C: (C) $Pb_2SSe_2^{2-}$; (E) $Pb_2STe_2^{2-}$; (F) $Pb_2Se_3^{2-}$; (G) $Pb_2Se_2Te^{2-}$; (H) $Pb_2SeTe_2^{2-}$; (I) $Pb_2Te_3^{2-}$; (J) Pb_2SSeTe^{2-}. Peaks labeled c, e, f, g, g_2, h, h_2, i, j, and j_2 denote ^{207}Pb satellites.

$$K_2Se + 2SnSe + 2(2,2,2\text{-crypt}) \xrightarrow[en]{2,2,2\text{-crypt}} 2(2,2,2\text{-crypt-}K^+) + Sn_2Se_3^{2-} \quad (1)$$

singlet at –436 ppm[2]) and was consistent with the relatively large amount of SnSe residue that remained when the solution was isolated. Single new ^{77}Se and ^{119}Sn (^{117}Sn) environments were observed, which were spin-coupled to one another (Figure 3). The satellite peak/central peak height ratios indicated that the Se environment is bonded to two equivalent tin atoms and that the Sn environment is bonded to three equivalent selenium atoms. In addition, the observation of satellites in the ^{119}Sn and ^{117}Sn NMR spectra arising from $J(^{117}Sn$–$^{119}Sn)$ coupling indicated the presence of two chemically equivalent tin atoms. These findings are consistent with the new trigonal bipyramidal $Sn_2Se_3^{2-}$ anion (structure II). Other Sn/Se anions were present in the solutions and are assigned to Sn(IV) species on the basis of the magnitudes of their $J(^{77}Se$–$^{119}Sn)$ coupling constants (1900–2100 Hz).[5]

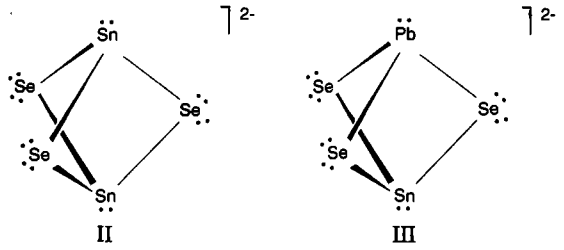

Analogous reactions among K_2Se, SnSe, and PbSe were conducted in en solvent in order to prepare the mixed-metal $SnPbSe_3^{2-}$ anion, which was obtained in sufficient concentration to allow full characterization by NMR spectroscopy when a 1:0.5:1.5 K_2Se/SnSe/PbSe mixture was extracted in en in the presence of 2,2,2-crypt. The ^{77}Se NMR spectrum showed that a large amount of unreacted Se^{2-} was still present in solution. Furthermore, the same species which had formed in the K_2Se/SnSe system

(5) Burns, R. C.; Devereux, L. A.; Granger, P.; Schrobilgen, G. J. *Inorg. Chem.* **1985**, *24*, 2615.
(6) Birchall, T.; Burns, R. C.; Devereux, L. A.; Schrobilgen, G. J. *Inorg. Chem.* **1985**, *24*, 890.

Table I. Chemical Shifts and Spin–Spin Coupling Constants for the $Pb_2S_nSe_{3-n}^{2-}$, $Pb_2S_nTe_{3-n}^{2-}$, and Pb_2SSeTe^{2-} Anions in en Solvent

anion	chemical shift, ppm			spin–spin coupling const, Hz[a]		reduced coupling const, $T^2\ J^{-1} \times 10^{20}$ [b]			
	^{207}Pb[c,d]	^{77}Se	^{125}Te	$^1J(^{77}Se–^{207}Pb)$	$^1J(^{125}Te–^{207}Pb)$	$^1K_{Se-Pb}$	$(^1K_{Se-Pb})_{RC}$	$^1K_{Te-Pb}$	$(^1K_{Te-Pb})_{RC}$
$Pb_2S_3^{2-}$	3533								
	(3534)								
$Pb_2S_2Se^{2-}$	3497	–17		98		20.3	5.71		
	(3498)	(–17)		(96)					
$Pb_2SSe_2^{2-}$	3421	–57		122		25.2	7.09		
	(3421)	(–58)		(124)					
$Pb_2Se_3^{2-}$	3302	–99		153		31.6	8.89		
	(3303)	(–99)		(152)					
$Pb_2S_2Te^{2-}$	3261		–589		818			122.7	27.69
	(3268)		(–591)		(818)				
Pb_2SSeTe^{2-}	3108	–147	–641	159	868	32.9	9.24	130.2	29.39
	(3104)								
$Pb_2STe_2^{2-}$	2671		–762		946			141.9	32.03
	(2666)		(–761)		(946)				
$Pb_2Te_3^{2-}$	1727		–928		1074			161.1	36.36
	(1728)		(–929)		(1074)				

[a] Measured at 31 °C. [b] Other equivalent SI units are N A^{-2} m^{-3}. [c] Values in parentheses are calculated from the equations given in Table III. [d] Pairwise additivity parameters (eq 1) for the ^{207}Pb chemical shifts: η_{SS} = 1178, η_{SSe} = 1160, η_{SeSe} = 1101, η_{STe} = 1045, η_{TeTe} = 576, and η_{SeTe} = 899 ppm. η_{SeTe} was calculated from data in ref 2.

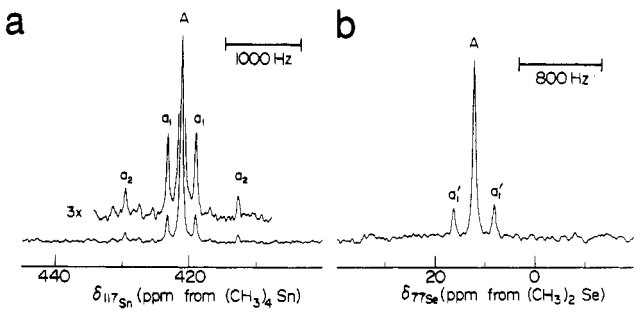

Figure 3. (a) ^{117}Sn NMR spectrum (89.128 MHz) and (b) ^{77}Se NMR spectrum (47.704 MHz) of the trigonal bipyramidal $Sn_2Se_3^{2-}$ anion (A) in en solvent. Peaks labeled a_1, a_1', and a_2 arise from $^1J(^{77}Se–^{117}Sn)$, $^1J(^{77}Se–^{117/119}Sn)$ (^{117}Sn and ^{119}Sn satellites not resolved), and $^2J(^{117}Sn–^{119}Sn)$ couplings, respectively.

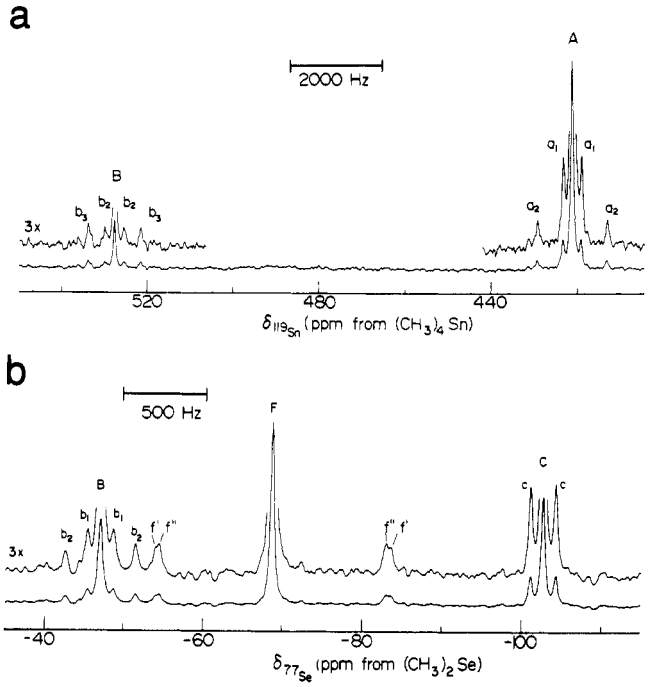

Figure 4. (a) ^{119}Sn NMR spectrum (93.276 MHz) and (b) ^{77}Se NMR spectra (47.704 MHz; 3 °C) resulting from the reaction of K_2Se with a 0.5:1.5 SnSe:PbSe mixture in en in the presence of 2,2,2-crypt: (A) $Sn_2Se_3^{2-}$; (B) $SnPbSe_3^{2-}$; (C) $Pb_2Se_3^{2-}$; (F) $SnSe_4^{4-}$. Peaks a_1 and b_2 arise from $^1J(^{77}Se–^{119}Sn)$ coupling and peaks b_1 and c from $^1J(^{77}Se–^{207}Pb)$ coupling. Peaks a_2 and b_3 arise from $^2J(^{117}Sn–^{119}Sn)$ and $^2J(^{119}Sn–^{207}Pb)$ couplings, respectively. The ^{119}Sn and ^{117}Sn satellites of $SnSe_4^{4-}$ are labeled f′ and f″, respectively.

were also present in solution along with the $Pb_2Se_3^{2-}$ anion. However, a new ^{119}Sn resonance, flanked by two pairs of satellites, was observed at 528 ppm (Figure 4a) which is assigned to $^1J(^{119}Sn–^{77}Se)$ and $^2J(^{119}Sn–^{207}Pb)$ of the trigonal bipyramidal $SnPbSe_3^{2-}$ anion (structure III). The ^{207}Pb chemical shift at 3439 ppm and the ^{77}Se chemical shift at –42 ppm (Figure 4b) are midway between those of $Sn_2Se_3^{2-}$ and $Pb_2Se_3^{2-}$, as expected for a homologous and isostructural series. The chemical shifts and spin–spin coupling constants for the $M_2Se_3^{2-}$ anions are given in Table II.

Interestingly, the ^{77}Se NMR resonances of the $M_2Se_3^{2-}$ anions were relatively broad at room temperature and broadened further at higher temperatures (53 °C). This broadening is possibly caused by an exchange of Se^{2-} with the trigonal bipyramidal anions by formation of an intermediate or low-energy transition state $M_2Se_4^{4-}$ species. The $M_2Se_4^{4-}$ anions are related to the known *cis*- and *trans*-$Sb_2Se_4^{2-}$ anions[7] and have been previously suggested as exchange intermediates for the $Pb_2Se_nTe_{3-n}^{2-}$ anions.[2] Other species present in the solution did not appear to be directly involved in the exchange processes as their peaks remained relatively sharp at higher temperatures.

The synthesis of the $Sn_2Te_3^{2-}$ was attempted in solution by the reaction of K_2Te with SnTe in en followed by addition of 2,2,2-crypt. However, ^{119}Sn and ^{125}Te NMR studies showed that Sn(IV)/Te anions were the major species formed, as suggested by the magnitudes of their $^1J(^{119}Sn–^{125}Te)$ coupling constants (2300–4500 Hz).[5] The structures of these anions could not be determined, but the magnitude of the $^1J(^{119}Sn–^{125}Te)$ coupling and the satellite/central peak ratios suggest that they contain trigonal planar $SnTe_3$ units. However, crystals of (2,2,2-crypt-$K^+)_2(Sn_2Te_3^{2-})$ were isolated from solutions resulting from reactions 2 and 3 and were characterized by X-ray crystallography

$$KSn_{0.53}S_{0.33}Te_{0.67} \xrightarrow[en]{2,2,2\text{-crypt}} (2,2,2\text{-crypt-}K^+)_2(Sn_2Te_3^{2-}) \quad (2)$$

$$K_2Te + 2SnTe \xrightarrow[NH_3(l)]{2,2,2\text{-crypt}} (2,2,2\text{-crypt-}K^+)_2(Sn_2Te_3^{2-}) \quad (3)$$

(see Crystal Structures). The difference between the two synthetic approaches could arise from a combination of chemical exchange processes involving Sn(IV)/Te anions and polytellurides and the

(7) Cordier, G.; Cook, R.; Schäfer, H. *Angew. Chem., Int. Ed. Engl.* **1980**, *19*, 324.

Table II. ^{77}Se, ^{119}Sn, and ^{207}Pb NMR Parameters for the $Sn_2Se_3^{2-}$, $SnPbSe_3^{2-}$, and $Pb_2Se_3^{2-}$ Anions in en Solvent

	chemical shift, ppm			coupling const, Hz			reduced coupling const, $T^2\,J^{-1} \times 10^{20}$			
anion	^{77}Se	^{119}Sn	^{207}Pb	^{77}Se–^{119}Sn	^{77}Se–^{207}Pb	M–M	$^1K_{M\text{-}Se}$	$(^1K_{M\text{-}Se})_{RC}$	$^2K_{M\text{-}M}$	$(^2K_{M\text{-}M})_{RC}$
$Sn_2Se_3^{2-}$	12	421		397		1514[a]	46.0	28.0	89.6	44.1
$SnPbSe_3^{2-}$	–42	528	3439	415	153	1145[b]	48.1 (Sn) 31.6 (Pb)	29.2 (Sn) 8.89 (Pb)	120.9	27.6
$Pb_2Se_3^{2-}$	–103		3290		153		31.6	8.89		

[a] $^2J(^{117}Sn$–$^{119}Sn)$. [b] $^2J(^{119}Sn$–$^{207}Pb)$.

Table III. Chalcogen Atom Substitution Trends in the Chemical Shifts and Spin–Spin Coupling Constants for the $Pb_2Ch_nCh'_{3-n}^{2-}$ (Ch/Ch' = S/Se, Se/Te, S/Te) Anions[a]

	chemical shift, ppm			$^1J(Ch$–$^{207}Pb)$, Hz	
anion	^{77}Se[b]	^{125}Te[b]	^{207}Pb[c]	^{77}Se–^{207}Pb	^{125}Te–^{207}Pb
$Pb_2S_nSe_{3-n}^{2-}$	$-99 + 41n$		$3303 + 139n - 21n^2$	$152 - 28n$	
$Pb_2Se_nTe_{3-n}^{2-}$ [d]	$-370 + 90n$	$-929 + 114n$	$1728 + 707n - 61n^2$	$266 - 39n$	$1071 - 78n$
$Pb_2S_nTe_{3-n}^{2-}$		$-929 + 169n$	$1728 + 1106n - 168n^2$		$1074 - 128n$

[a] n is the number of lighter chalcogen atoms. [b] The equation represents the best linear fit of three data points. [c] Calculated from eq 2 and the pairwise additivity parameters, η, given in Table I. [d] Calculated from data in ref 2.

low solubility of $(2,2,2\text{-crypt-}K^+)_2(Sn_2Te_3^{2-})$. Corbett[8] has noted that a large number of 2,2,2-crypt polyanion salts isolated and structurally characterized by X-ray crystallography have low solubilities in en and are easily crystallized. However, the isolated crystalline material may not be representative of the major species in solution. The trigonal planar thallium(III) anion $TlCh_3^{3-}$ (Ch = Se, Te) is an exemplary case and could only be identified in solution by NMR spectroscopy[5] even though the thallium(I) anion $Tl_2Te_2^{2-}$ crystallized from the same solution and was characterized in the solid state by X-ray crystallography.[9]

Chemical Shift Trends. Additivity among chemical shifts for homologous series of classically bonded main-group chalcogenide anions appears to be a consistent feature.[2,5,10] As in a previous study of the $Pb_2Se_nTe_{3-n}^{2-}$ anion series, the ^{77}Se and ^{125}Te chemical shifts and the one-bond spin–spin coupling constants $^1J(^{77}Se$-$^{207}Pb)$ and $^1J(^{125}Te$-$^{207}Pb)$ for the new $Pb_2S_nSe_{3-n}^{2-}$ and $Pb_2S_nTe_{3-n}^{2-}$ anion series were found to be directly additive and to be linear functions of the number of sulfur atoms in each series. The linear dependences obtained from least-squares analyses are given in Table III.

The ^{207}Pb chemical shifts for the new series, however, showed pairwise additivity dependences; i.e., the differences between successive $\delta(^{207}Pb)$ values in each series decreased linearly with the number of sulfur atoms. The possibility of pairwise additivity in the previously reported $Pb_2Se_nTe_{3-n}^{2-}$ series[2] was not considered in the earlier study but has been demonstrated in the present study.

Kidd and Spinney[11] analyzed ^{121}Sb NMR chemical shifts for the mixed-halide anions $SbCl_nBr_{6-n}^-$ by considering the number of similar edges of the octahedron formed by the halogen atoms. Similarly, one can fit the ^{207}Pb chemical shifts of the $Pb_2Ch_nCh'_{3-n}^{2-}$ (Ch/Ch' = S/Se, Se/Te, and S/Te) anion series using eq 4, where η is a pairwise additivity parameter representing

$$\delta(^{207}Pb) = {}^1/_2(n-1)n\eta_{ChCh} + n(3-n)\eta_{ChCh'} + {}^1/_2(2-n)(3-n)\eta_{Ch'Ch'} \quad (4)$$

the type of equatorial edge and n is the number of lightest chalcogen atoms ($n \leq 3$). The second-order dependence of the ^{207}Pb chemical shifts on n is made more evident by rearranging eq 4 to give eq 5. The values for the direct additivity parameters, η, are listed in Table I (footnote *d*) along with their equations. The equations and values for the direct additivity parameters are given in Table III. As can be seen from Table I, there is excellent agreement between the calculated and measured NMR parameters of all the dileadtrichalcogenide anions.

$$\delta(^{207}Pb) = 3\eta_{Ch'Ch'} + {}^1/_2[6\eta_{ChCh'} - (\eta_{ChCh} + 5\eta_{Ch'Ch'})]n - {}^1/_2[2\eta_{ChCh'} - (\eta_{ChCh} + \eta_{Ch'Ch'})]n^2 \quad (5)$$

A comparison among appropriate parameters for the $Pb_2Ch_3^{2-}$ series in Table III reveals that the values of the slopes and curvatures (^{207}Pb chemical shifts) decrease upon chalcogen atom substitution in the following order: S → Te > Se → Te ≫ S → Se, correlating with Pauling's electronegativity ordering: χ_S (2.5) > χ_{Se} (2.4) ≫ χ_{Te} (2.1).[12] The observed trend can therefore be rationalized on the basis that the greater difference in electronegativity between the substituted chalcogen atoms should perturb the electronic structure of the trigonal bipyramidal anion more and have a correspondingly greater influence on its NMR parameters. The extreme high-frequency (low-field) shift has previously been noted by Elund *et al.* as possibly being due to the HAHA effect (heavy-atom shift of the heavy atom)[13,14] on the basis of relativistic extended Hückel calculations on PbH_3^-. A similar effect is likely to be operative for the ^{207}Pb chemical shifts of the series of dileadtrichalcogenide anions reported here and previously.[2]

In a previous study[2] it was found that the ^{207}Pb chemical shifts of the $Pb_2Se_3^{2-}$ and $Pb(SePh)_3^-$ anions[15,16] are very similar and consistent with the near-identical geometries of the pyramidal $PbSe_3$ moieties determined by X-ray crystallography.[2] However, the ^{119}Sn chemical shifts of the $Sn_2Se_3^{2-}$ (421 ppm) and $SnPbSe_3^{2-}$ (528 ppm) anions differ significantly from that of $Sn(SePh)_3^-$ [$\delta(^{119}Sn)$ 208 ppm][16,17] despite the similar geometries of their pyramidal $SnSe_3$ moieties (see Crystal Structures). At present no explanation can be offered for this difference.

Coupling Constants (^1J, ^1K, and Relativistically Corrected $^1K_{RC}$). In order to look at structurally related effects on the spin–spin coupling, the nuclear-independent reduced coupling constant, $^nK_{AB}$, gives a better representation of electronic environments in the series of anions under discussion. Furthermore, Pyykkö and Wiesenfeld[18] have shown that relativistic effects on the Fermi contact term (s-electron density) dominate $^nK_{AB}$ for the heavy main-group elements. A method has been suggested to correct

(8) Corbett, J. D. *Chem. Rev.* **1985**, *85*, 383.
(9) Burns, R. C.; Corbett, J. D. *J. Am. Chem. Soc.* **1981**, *103*, 2627.
(10) Björgvinsson, M.; Sawyer, J. F.; Schrobilgen, G. J. *Inorg. Chem.* **1991**, *30*, 4238.
(11) Kidd, R. G.; Spinney, H. G. *Inorg. Chem.* **1972**, *12*, 1967.
(12) Pauling, L. *The Nature of the Chemical Bond*, 3rd ed.; Cornell University Press: Ithaca, NY, 1960; Chapter 3, p 93.
(13) Pyykkö, P.; Görling, A.; Rösch, N. *Mol. Phys.* **1987**, *61*, 195.
(14) Elund, U.; Lejon, T.; Pyykkö, P.; Venkatachalam, T.; Buncel, E. *J. Am. Chem. Soc.* **1987**, *109*, 5982.
(15) Arsenault, J. J. I.; Dean, P. A. W. *Can. J. Chem.* **1983**, *61*, 1516.
(16) Dean, P. A. W.; Payne, N. C.; Vittal, J. J. *Inorg. Chem.* **1984**, *23*, 4232.
(17) Dean, P. A. W.; Payne, N. C.; Vittal, J. *Can. J. Chem.* **1985**, *63*, 394.
(18) Pyykkö, P.; Wiesenfeld, L. *Mol. Phys.* **1981**, *43*, 557.

Table IV. Summary of Crystal Data and Refinement Results for (2,2,2-crypt-K^+)$_2$$Sn_2Ch_3^{2-}$ (Ch = Te, Se)

	$Sn_2Te_3^{2-}$ (−100 °C)	$Sn_2Te_3^{2-}$ (24 °C)	$Sn_2Se_3^{2-}$ (24 °C)
formula	$C_{36}H_{72}K_2N_4O_{12}Sn_2Te_3$	$C_{36}H_{72}K_2N_4O_{12}Sn_2Te_3$	$C_{36}H_{72}K_2N_4O_{12}Sn_2Se_3$
a, Å	11.703(4)	11.817(7)	10.342(3)
b, Å	11.703(4)	11.817(7)	46.976(6)
c, Å	21.945(6)	22.01(2)	11.402(4)
α, deg	90.0	90.0	90.0
β, deg	90.0	90.0	90.15(3)
γ, deg	120.0	120.0	90.0
V, Å^3	2603(1)	2662(5)	5539(3)
Z	2	2	4
T, °C	−100	24	24
color	red	red	yellow
fw	1451.4	1451.4	1305.44
space group	$P\bar{3}c1$	$P\bar{3}c1$	$P2_1/n$
ρ_{calcd}, g cm^{-3}	18.52	18.11	15.65
μ, cm^{-1}	28.22	27.60	30.7
λ, Å	0.710 73 (Mo Kα)	0.560 86 (Ag Kα)	0.710 73 (Mo Kα)
R (R_w)	0.0628 (0.0711)	0.102 (0.116)	0.090 (0.077)

for the relativistic effect.[5] The relativistic correction is accomplished by dividing $^nK_{AB}$, as defined in ref 19, by $(|\psi_{ns}(0)|^2)_{rel}/(|\psi_{ns}(0)|^2)_{nonrel}$ for both spin–spin-coupled elements A and B to obtain the relativistically corrected reduced coupling constant, $(^nK_{AB})_{RC}$. The following ratios for $(|\psi_{ns}(0)|^2)_{rel}/(|\psi_{ns}(0)|^2)_{nonrel}$ are obtained from ref 18: Pb, 3.079; Te, 1.439; Sn, 1.425; Se, 1.155. The reduced coupling constants, $^1K_{M-Ch}$, and relativistically corrected reduced coupling constants, $(^1K_{M-Ch})_{RC}$, are given in Tables I and II.

As noted in a previous study of the $Pb_2Se_nTe_{3-n}^{2-}$ series,[2] there is again a large disparity (200–540%) between $(^1K_{Pb-Se})_{RC}$ and $(^1K_{Pb-Te})_{RC}$ values in the $Pb_2S_nSe_{3-n}^{2-}$ and $Pb_2S_nTe_{3-n}^{2-}$ anion series and the Pb_2SSeTe^{2-} anion despite relativistic corrections. This contrasts with the $(^1K_{M-Ch})_{RC}$ values of the series of sp^2-hybridized $SnCh_3^{2-}$ and $TlCh_3^{3-}$ anions and sp^3-hybridized $SnCh_4^{4-}$ anions, whose $(^1K_{M'-Ch})_{RC}$ values are approximately 3–20 times greater than those for the $M_2Ch_3^{2-}$ anions, and is consistent with the dominant use of p orbital bonding in the $M_2Ch_3^{2-}$ anions.[5] Moreover, the disparity between values of $(^1K_{M-Ch})_{RC}$ for the selenium and tellurium parameters of a given mononuclear Sn or Tl anion series seldom exceeds 30%. The values for $(^1K_{Sn-Se})_{RC}$ and $(^1K_{Pb-Se})_{RC}$ in $SnPbSe_3^{2-}$ are essentially identical to those of the ditin and dilead analogs (Table II), whereas the values of $(^1K_{Sn-Se})_{RC}$ are approximately 3 times those of $(^1K_{Pb-Se})_{RC}$.

The greatly diminished s characters of the M–Ch bonds in the $M_2Ch_3^{2-}$ anions are consistent with the relative inertness of the M(II) atom valence s electrons and their large contribution to the M(II) atom lone pair. Furthermore, the dominant use of p orbitals for skeletal bonding is to be expected from the previously noted cluster-like character of the $Pb_2Se_3^{2-}$ and $Pb_2Te_3^{2-}$ anions.[2,3] This is reflected in the small M–Ch–M (~70%) and Ch–M–Ch (~90°) bond angles of the $Sn_2Se_3^{2-}$ and $Sn_2Te_3^{2-}$ anions, which also suggest that p orbitals are predominantly used in the cage bonding (see Crystal Structures). The dominant p character of the M–Ch bonds in the $M_2Ch_3^{2-}$ anion clusters could be responsible for the notably smaller $^1J(^{77}Se-^{119}Sn)$ coupling constants for $Sn_2Se_3^{2-}$ (397 Hz) and $SnPbSe_3^{2-}$ (415 Hz) as compared to the pyramidal $Sn(SePh)_3^-$ anion (710 Hz).[15]

The spin–spin couplings between the axial atoms of the $Sn_2Se_3^{2-}$ and $SnPbSe_3^{2-}$ anions are the first Sn(II)–Sn(II) and Sn(II)–Pb(II) couplings to be observed. The $^2J(^{117}Sn-^{119}Sn)$ coupling constant is greater than the two-bond coupling constants between selenium-bridged Sn(IV) atoms (100–350 Hz),[20,21] but it is significantly less than one-bond $^{119}Sn(IV)-^{119}Sn(IV)$ coupling constants (900–4000 Hz and up to 15 000 Hz).[22] In general, the values and signs of $^2J(^{119}Sn-^{117}Sn)$ for Sn–Z–Sn units are known to be dependent on the bridging Z atom and the Sn–Z–Sn bond angle as well as on the chemical environments of the spin–spin-coupled tin atoms.[20,21] However, the relative importance of each factor is not known. Owing to a lack of data for Sn(II)–Sn(II) and Sn(II)–Pb(II) coupling constants, it is not possible at present to assess on the basis of the metal–metal coupling alone whether or not the relatively large values of $^2J(^{117}Sn-^{119}Sn)$ and $^2J(^{207}Pb-^{119}Sn)$ for $Sn_2Se_3^{2-}$ and $SnPbSe_3^{2-}$ signify bonding interactions between the axial metal atoms. Owing to the proximity of the two axial tin/lead atoms (see Crystal Structures and refs 2 and 3), the relatively large values for the coupling constants could be the result of a high electron-spin correlation between valence s-electron pairs of the axial metal atoms.

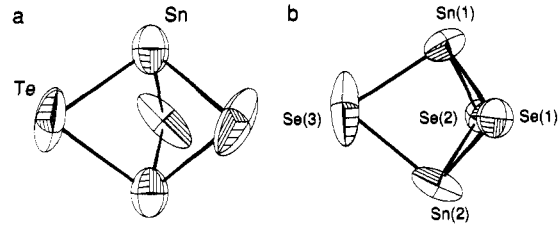

Figure 5. ORTEP diagrams of the (a) $Sn_2Te_3^{2-}$ (24 °C) and (b) $Sn_2Se_3^{2-}$ anions including the atom-numbering scheme with ellipsoids drawn at 50% probability.

X-ray Crystal Structures of (2,2,2-crypt-K^+)$_2$($Sn_2Te_3^{2-}$) and (2,2,2-crypt-K^+)$_2$($Sn_2Se_3^{2-}$). The crystal structures of the title compounds consist of well-separated cryptated potassium ions and $Sn_2Te_3^{2-}$ and $Sn_2Se_3^{2-}$ anions. Details of the data collection parameters and other crystallographic information are given in Table IV. The final atomic coordinates and the equivalent isotropic thermal parameters for the non-hydrogen atoms are summarized in Table V. All relevant bond distances and angles for the $Sn_2Te_3^{2-}$ and $Sn_2Se_3^{2-}$ anions are given in Table VI.

The most interesting aspect of the structures is the flattened trigonal bipyramidal shape of the anions (Figures 5 and 6) which makes them isostructural with their dilead analogs.[2,3] The centric space group of (2,2,2-crypt-K^+)$_2$($Sn_2Te_3^{2-}$) requires that $Sn_2Te_3^{2-}$ have D_{3h} symmetry, while that for $Sn_2Se_3^{2-}$ only restricts it to C_{2h} symmetry. However, minor differences in bond lengths and angles are such that $Sn_2Se_3^{2-}$ can also be properly classified as D_{3h}, as was found for the dilead analogs. The Sn atoms are in apical positions and the Te and Se atoms in equatorial positions, in agreement with the structure deduced from the solution NMR study of $Sn_2Se_3^{2-}$. In both the $Sn_2Te_3^{2-}$ and $Sn_2Se_3^{2-}$ anions, the tin and chalcogen atoms occupy the same site symmetries as their lead analogs, which have been recently solved in the same respective space groups, and exhibit remarkably similar thermal ellipsoid distributions. As noted before in the $Pb_2Te_3^{2-}$ [3] and

(19) Pople, J. A.; Santry, D. P. *Mol. Phys.* **1964**, *8*, 1.
(20) Blecher, A.; Mathiasch, B.; Mitchell, T. N. *J. Organomet. Chem.* **1980**, *184*, 175.
(21) Puff, H.; Friedrichs, E.; Hundt, R.; Zimmer, R. *J. Organomet. Chem.* **1983**, *259*, 79.
(22) Wrackmeyer, B. *Annu. Rep. NMR Spectrosc.* **1985**, *16*, 73.

Table V. Atomic Coordinates and Equivalent Isotropic Displacement Coefficients for $(2,2,2\text{-crypt-K}^+)_2Sn_2Ch_3^{2-}$ (Ch = Te, Se)

$Sn_2Te_3^{2-}$ (−100 °C)

	x	y	z	U(eq),[a] Å²		x	y	z	U(eq),[a] Å²
Sn	0.0	0.0	0.1755(1)	0.086(1)	C(3)	0.3614(11)	0.2582(11)	0.0944(5)	0.026(6)
Te	0.1846(2)	−0.0313(3)	0.2358(1)	0.059(2)	C(4)	0.3354(11)	0.2592(11)	0.0280(4)	0.024(5)
K	0.6667	0.3333	0.0508(2)	0.019(1)	O(2)	0.4340(7)	0.2513(7)	−0.0062(3)	0.019(3)
N(1)	0.6667	0.3333	0.1841(7)	0.031(6)	C(5)	0.4329(11)	0.2835(11)	−0.0696(5)	0.025(3)
C(1)	0.5416(12)	0.3242(13)	0.2054(5)	0.034(6)	C(6)	0.5296(10)	0.2565(11)	−0.1037(4)	0.025(6)
C(2)	0.5010(12)	0.4097(12)	0.1723(5)	0.029(6)	N(2)	0.6667	0.3333	−0.0824(6)	0.018(5)
O(1)	0.4800(7)	0.3789(7)	0.1076(3)	0.021(4)					

$Sn_2Te_3^{2-}$ (24 °C)

	x	y	z	U(eq),[a] Å²		x	y	z	U(eq),[a] Å²
Sn	0.0	0.0	0.1753(4)	0.098(4)	C(3)	0.739(6)	0.104(6)	0.086(3)	0.107(24)
Te	0.2009(6)	0.0	0.2500	0.158(6)	C(4)	0.735(5)	0.078(5)	0.030(2)	0.067(17)
K	0.6667	0.3333	0.0497(6)	0.033(6)	O(2)	0.748(3)	0.185(3)	−0.011(1)	0.049(10)
N(1)	0.6667	0.3333	0.175(3)	0.039(18)	C(5)	0.714(4)	0.150(4)	−0.065(2)	0.031(13)
C(1)	0.671(6)	0.224(6)	0.207(2)	0.113(25)	C(6)	0.744(6)	0.274(6)	−0.108(2)	0.092(19)
C(2)	0.598(4)	0.102(4)	0.167(2)	0.047(15)	N(2)	0.6667	0.3333	−0.081(3)	0.039(18)
O(1)	0.625(3)	0.102(3)	0.1067(2)	0.071(11)					

$Sn_2Se_3^{2-}$ (24 °C)

	x	y	z	U(eq),[a] Å²		x	y	z	U(eq),[a] Å²
Sn(1)	5265(2)	1207(1)	6358(2)	70(1)	C(25)	−573(26)	1939(7)	−963(20)	75(9)
Sn(2)	8244(2)	1159(1)	6312(2)	87(1)	C(26)	649(26)	1909(7)	−1694(21)	74(9)
Se(1)	6829(3)	1400(1)	8006(2)	59(1)	K(2)	1733(6)	569(1)	1277(5)	44(2)
Se(2)	6791(3)	1402(1)	4660(2)	59(1)	N(100)	3364(21)	577(5)	−900(16)	62(7)
Se(3)	6586(6)	727(1)	6308(3)	147(2)	C(101)	3962(28)	289(7)	−1089(23)	80(9)
K(1)	1824(6)	2069(1)	1381(5)	46(2)	C(102)	3060(29)	59(7)	−825(23)	89(11)
N(1)	1954(23)	2050(6)	4096(18)	71(7)	O(103)	2670(18)	42(4)	312(15)	74(6)
C(1)	2079(31)	2331(8)	4505(25)	102(12)	C(104)	1792(37)	−171(9)	622(32)	146(16)
C(2)	1462(29)	2560(7)	3853(22)	92(11)	C(105)	1508(35)	−212(8)	1700(28)	127(14)
O(3)	2002(18)	2583(4)	2698(15)	75(6)	O(106)	639(19)	35(5)	1949(17)	86(6)
C(4)	1448(31)	2828(8)	2040(24)	102(11)	C(107)	284(31)	30(8)	3119(26)	105(12)
C(5)	2109(31)	2846(8)	909(25)	108(12)	C(108)	−528(27)	265(7)	3480(22)	77(10)
C(7)	2227(31)	2597(8)	−897(23)	101(11)	N(110)	49(20)	560(5)	3431(16)	57(7)
C(8)	1450(29)	2376(7)	−1700(23)	88(10)	C(111)	−949(25)	796(6)	3305(19)	59(8)
O(6)	1676(17)	2588(5)	207(15)	79(6)	C(112)	−1495(26)	823(7)	2141(19)	68(9)
N(10)	1744(21)	2087(5)	−1319(16)	60(6)	O(113)	−510(15)	890(4)	1378(12)	50(5)
C(11)	2996(27)	1956(7)	−1729(21)	77(10)	C(114)	−1102(28)	968(7)	306(21)	91(11)
C(12)	3575(27)	1730(7)	−1074(21)	83(10)	C(115)	6(26)	1061(7)	−539(21)	78(9)
O(13)	3835(18)	1842(4)	53(14)	70(6)	O(116)	860(17)	827(4)	−802(13)	63(5)
C(14)	4594(31)	1655(8)	671(24)	96(11)	C(117)	1707(24)	912(6)	−1745(19)	60(8)
C(15)	4932(30)	1742(8)	1762(23)	99(11)	C(118)	2600(23)	649(6)	−1888(19)	52(8)
O(16)	3834(18)	1785(4)	2492(14)	74(6)	C(119)	4442(28)	770(7)	−821(22)	78(10)
C(17)	4147(29)	1861(7)	3624(21)	87(10)	C(120)	5010(31)	791(8)	537(23)	108(12)
C(18)	3061(26)	1847(7)	4389(24)	80(10)	O(121)	4121(16)	877(4)	1353(14)	61(5)
C(19)	748(29)	1944(7)	4541(23)	89(11)	C(122)	4651(25)	888(6)	2464(20)	69(9)
C(20)	106(28)	1713(7)	3742(21)	75(9)	C(123)	3780(29)	960(7)	3271(24)	93(11)
O(21)	−238(17)	1847(4)	2686(14)	68(6)	O(124)	2773(18)	757(4)	3402(14)	68(6)
C(22)	−1065(27)	1670(7)	1984(21)	78(9)	C(125)	1969(29)	811(7)	4296(24)	88(11)
C(23)	−1437(29)	1786(8)	884(22)	96(11)	C(126)	938(27)	568(7)	4451(22)	86(10)
O(24)	−287(18)	1829(4)	181(14)	72(6)					

[a] Equivalent isotropic U defined as one-third of the trace of the orthogonalized U_{ij} tensor.

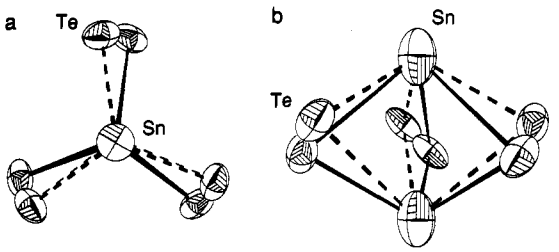

Figure 6. ORTEP diagram of the $Sn_2Te_3^{2-}$ (−100 °C) anion viewed (a) along the C_3 axis and (b) perpendicular to the C_3 axis, showing the disorder in the equatorial plane. Ellipsoids are drawn at 50% probability.

$Pb_2Se_3^{2-}$ [2] anions, the impeller shape of the equatorial Te ellipsoids at room temperature (Figure 5a) and one of the equatorial Se ellipsoids (Figure 5b) seems unusual and it had been proposed that it was probably due to a slight static disorder of the anions. Static disorders have also been noted at room temperature for the Pb_5^{2-} and Sn_5^{2-} anions.[23]

In the case of the $Sn_2Te_3^{2-}$ anion, the apical tin atoms exhibit elongated thermal ellipsoids similar to their waist tellurium atoms. Confirmation and resolution of the disorder were obtained by recording a data set at −100 °C (Figure 6). The disorder involves two $Sn_2Te_3^{2-}$ ions of D_{3h} symmetry oriented equally "up" and "down" and displaced by about 0.028 Å along the C_3 axis. Although the disorder for the equatorial Te atoms could be resolved, giving rise to normal thermal parameters (Table V), the disorder on the apical tin atoms could not be resolved even at −100 °C because the two sites were too close. Consequently, the distances and angles presented in Table VI for $Sn_2Te_3^{2-}$ at −100 °C are average values.

The $Sn_2Se_3^{2-}$ anion is similar to the $Pb_2Se_3^{2-}$ anion[2] in that only one of the Se ellipsoids possesses an impeller shape while the other two Se ellipsoids are nearly spherical. It should also be noted that in both the tin and lead structures the metal ellipsoids are slightly elongated toward the anisotropic Se atom. The strict

(23) Edwards, P. A.; Corbett, J. D. *Inorg. Chem.* **1977**, *16*, 903.

Table VI. Selected Bond Lengths (Å) and Bond Angles (deg) in the $Sn_2Te_3^{2-}$ and $Sn_2Se_3^{2-}$ Anions

	$Sn_2Te_3^{2-}$ (−100 °C)		$Sn_2Te_3^{2-}$ (24 °C)
	Bond Lengths		
Sn···Sn	3.270(6)[a]		3.287(17)
Sn–Te	2.887(4)[a]		2.887(8)
	Bond Angles		
Sn–Te–Sn	68.7(1)[a]		69.4(3)
Te–Sn–Te	90.9(1)[a]		90.8(2)
	$Sn_2Se_3^{2-}$		
	Bond Lengths		
Sn(1)···Sn(2)	3.090(3)	Sn(2)–Se(1)	2.677(3)
Sn(1)–Se(1)	2.637(3)	Sn(2)–Se(2)	2.662(4)
Sn(1)–Se(2)	2.663(3)	Sn(2)–Se(3)	2.658(6)
Sn(1)–Se(3)	2.639(5)		
	Bond Angles		
Se(1)–Sn(1)–Se(2)	92.1(1)	Se(2)–Sn(2)–Se(3)	87.9(1)
Se(1)–Sn(1)–Se(3)	89.6(1)	Sn(1)–Se(1)–Sn(2)	71.1(1)
Se(2)–Sn(1)–Se(3)	88.3(1)	Sn(1)–Se(2)–Sn(2)	70.9(1)
Se(1)–Sn(2)–Se(2)	91.2(1)	Sn(1)–Se(3)–Sn(2)	71.4(1)
Se(1)–Sn(2)–Se(3)	88.3(1)		

[a] Average values.

analogy of these unusual features in both structures tends to suggest that the anisotropy is related not to a simple static disorder but rather to a packing effect. Indeed, a close examination of the shortest anion–cation contacts shows that they are somewhat shorter for Se(1) and Se(2) (3.808 and 3.675 Å, respectively) than for Se(3) (3.857 Å) (van der Waals contact Se···CH_2 = 4.0 Å).[4] In other words, the longer contacts between Se(3) and a CH_2 group would allow this selenium atom to exhibit a rocking motion about an axis defined by the two spherical selenium atoms. This rocking motion is also manifested by the elongated thermal ellipsoids of Sn(1) and Sn(2), which also have long contacts with the adjacent cryptand (the shortest Sn(1)···CH_2 and Sn(2)···CH_2 contacts are 3.911 and 3.921 Å, respectively; sum of van der Waals radii 4.2 Å[4]) and are elongated toward Se(3).

In both anion structures, the Sn···Sn distances [$Sn_2Te_3^{2-}$, 3.270(6) Å (−100 °C), 3.287(17) Å (24 °C), $Sn_2Se_3^{2-}$, 3.096(3) Å] are significantly less than the approximate van der Waals distance (4.4 Å)[4] and 0.31–0.42 Å greater than the single Sn–Sn bond distance (2.80 Å, α-tin)[24] and shortest Sn···Sn distances in the structurally related homopolyatomic anion Sn_5^{2-} (equatorial–equatorial distances 3.095(10) Å; equatorial–axial distances 2.877(7) Å; axial–axial distance 4.481 Å).[23] Moreover, the shortest Sn···Sn distances in other species range from 2.764(2) to 3.353(3) Å.[25] Short metal–metal distances have also been noted in the isostructural $Pb_2Te_3^{2-}$ (3.247 Å)[3] and $Pb_2Se_3^{2-}$ (3.184 Å)[2] anions (van der Waals contact for Pb···Pb 4.0 Å),[4] and as in the present case, the Pb···Pb distance is greater in $Pb_2Te_3^{2-}$ than in the selenide anion. Although comparisons of the M···M distances and the corresponding van der Waals contacts show that the differences between these values are smaller in the tin anions, suggesting more compressed trigonal bipyramids, this may, in large measure, be due to uncertainties in the van der Waals distances used. However, the ratio of cryptated potassium to anions in the unit cell and the chemical shifts in the ^{119}Sn and ^{207}Pb NMR spectra show that the axial metals are in the +2 oxidation state and therefore would not be expected to have a fourth bonding interaction such as a metal–metal bond. This short metal–metal distance is likely caused by geometric constraints inherent in the trigonal bipyramidal structures.

While the Sn···Sn distances are significantly less than the van der Waals contacts, the equatorial Te···Te distances (−100 °C, 4.103 Å; 24 °C, 4.111 Å) and Se···Se distances (3.741 Å) are only marginally smaller than or equal to the van der Waals contact distances (4.2 and 3.8 Å, respectively)[4] and are in accord with a localized valence-bond structure. The present Te···Te and Se···Se distances are in fact slightly smaller than those in their dilead analogs (4.25 Å in $Pb_2Te_3^{2-}$; 3.88 Å in $Pb_2Se_3^{2-}$).

The Sn–Te distance in the $Sn_2Te_3^{2-}$ anion is 2.887(4) Å (−100 °C) and 2.887(8) Å (24 °C), compared with an average Sn–Se bond length of 2.656(4) Å, while the Te–Sn–Te angles [−100 °C, 90.9(1)° × 6; 24 °C, 90.8(2)° × 6] are larger than the corresponding Se–Sn–Se bond angles [average 89.6(1)°; range 87.9(1)–92.1(1)°] and the Sn–Te–Sn bond angles [−100 °C, 68.7(1)° × 3; 24 °C, 69.4(3)° × 3] are correspondingly smaller than the analogous Sn–Se–Sn angles [average 71.1(1)°; range 70.9(1)–71.4(1)°]. As already pointed out for the $Pb_2Ch_3^{2-}$ anions,[2,3] the angle trends in $Sn_2Se_3^{2-}$ and $Sn_2Te_3^{2-}$, namely, Se–Sn–Se < Te–Sn–Te and Sn–Se–Sn > Sn–Te–Sn, can be rationalized on the basis of the electronegativity difference between Se and Te. As one would expect from the VSEPR rules,[26] the Ch–Sn–Ch bond angle decreases and the corresponding Sn–Ch–Sn bond angle increases with the more electronegative chalcogen atom. Little or no information is available in the literature regarding Sn(II)–Te and Sn(II)–Se bond distances. The Sn–Te distances (−100 °C, 2.887(4) Å; 24 °C, 2.887(8) Å) are, however, substantially longer than the Sn(IV)–Te bond distances in $Sn_2Te_7^{4-}$ [2.683(2) Å, terminal; 2.804(2) Å, bridge],[27] $Sn_2Te_6^{4-}$ [2.695(1) Å, terminal; 2.799(1) Å, bridge],[28] and $SnTe_4^{4-}$ (2.75 Å),[29] as well as the sum of the covalent radii, 2.77 Å (1.37 Å for Te; 1.40 Å for Sn).[24] The Sn–Te distance is, however, in better agreement with the sum of the Te covalent radius and the metallic radius of Sn(II) (1.434 Å):[30] 2.80 Å. Similarly, the Sn(II)–Se distances in $Sn_2Se_3^{2-}$ [which vary widely from 2.637(3) to 2.677(3) Å due to the anisotropy in the thermal parameters of the Sn and Se atoms] are longer than the sum of the covalent radii (2.57 Å)[24] and the Sn(IV)–Se single bond distances in $Sn_2Se_6^{4-}$ [2.458(2) Å, terminal; 2.605(2) Å, bridge],[31] and in $Na_4SnSe_4 \cdot 16H_2O$ [average, 2.519(2) Å],[32] but somewhat shorter than the Sn(IV)–Se distances in $Sn(Se_4)_3^{2-}$ [average, 2.709(3) Å].[33] The Sn(II)–Se distances of $Sn_2Se_3^{2-}$ are similar to those of the $SnSe_3$-pyramide in $Sn(SePh)_3^-$ [2.649(1) Å × 2 and 2.671(1) Å].[27] The average pyramidal Se–Sn–Se angle of $Sn(SePh)_3^-$ is 91.91(3)° and is only slightly larger than the average Se–Sn–Se angle in $Sn_2Se_3^{2-}$ of 89.6(1)°.

(24) Pauling, L. *The Nature of the Chemical Bond*, 3rd ed.; Cornell University Press: Ithaca, NY, 1960; Chapter 3, pp 224–225.
(25) The shortest Sn···Sn distances are given in square brackets for the following. (a) Ph_6Sn_2 [2.770(4) Å]: von Preut, H.; Haput, H. J.; Huber, F. *Z. Anorg. Allg. Chem.* **1973**, *396*, 81. (b) $[(CH_3)_3Si]_2HCSnCH[Si(CH_3)_3]_2$ dimer [2.764(2) Å]: Goldberg, D. E.; Harris, D. H.; Lappert, M. F.; Thomas, K. M. *J. Chem. Soc., Chem. Commun.* **1976**, 261. (c) Sn_8R_8 (R = 2,6-diethylphenyl) [2.839(2)–2.864(2) Å]: Sita, L. R.; Kinoshita, I. *Organometallics* **1990**, *9*, 2865. (d) Sn_4^{2-} [2.934(3) – 2.972(7) Å]: Critchlow, S. C.; Corbett, J. D. *J. Chem. Soc., Chem. Commun.* **1981**, 236. (e) Sn_9^{4-} [2.928(6)–3.308(5) Å]: Corbett, J. D.; Edwards, P. A. *J. Am. Chem. Soc.* **1977**, *99*, 3313. (f) Sn_9^{3-} [2.923–3.315 Å]: Critchlow, S. C.; Corbett, J. D. *J. Am. Chem. Soc.* **1983**, *105*, 5715. (g) $TlSn_8^{3-}$ [2.879(4)–3.301(5) Å] and $TlSn_9^{3-}$ [2.862(3)–3.353(3) Å]: Burns, R. C.; Corbett, J. D. *J. Am. Chem. Soc.* **1982**, *104*, 2804.
(26) Gillespie, R. J.; Hargittai, I. *The VSEPR Model of Molecular Geometry*; Allyn and Bacon: Boston, MA, 1991.
(27) Brinkmann, C.; Eisenmann, B.; Schäfer, H. *Mater. Res. Bull.* **1985**, *20*, 299.
(28) Huffman, J. C.; Haushalter, J. P.; Umarji, A. M.; Shenoy, G. K.; Haushalter, R. C. *Inorg. Chem.* **1984**, *23*, 2312.
(29) Eisenmann, B.; Schäfer, H.; Schrod, H. *Z. Naturforsch.* **1983**, *38B*, 921.
(30) Pauling, L. *The Nature of the Chemical Bond*, 3rd ed.; Cornell University Press: Ithaca, NY, 1960; Chapter 3, p 420.
(31) Devereux, L. A.; DiCiommo, D. A.; Mercier, H. P. A.; Schrobilgen, G. J. Unpublished work.
(32) von Krebs, B.; Hürter, H. U. *Z. Anorg. Allg. Chem.* **1980**, *462*, 143.
(33) Huang, S. P.; Dhingra, S.; Kanatzidis, M. G. *Polyhedron* **1990**, *9*, 1389.

The structures of the cations are similar to those determined previously in (2,2,2-crypt-K^+)$_2Tl_2Te_2^{2-}$·en,[9] (2,2,2-crypt-K^+)$_2Pb_2Se_3^{2-}$,[2] (2,2,2-crypt-K^+)$_2Pb_2Te_3^{2-}$,[3] and (2,2,2-crypt-K^+)$_2Te_3^{2-}$·en[34] (K···O and K···N distances are given in supplementary Table IX; they are in the ranges 2.70(1)–2.93(2) [2.73(4)–2.87(6)] Å with the $Sn_2Te_3^{2-}$ anions and 2.77(2)–3.10(2) Å with the $Sn_2Se_3^{2-}$ anion).

Bonding in $Pb_2S_nCh_{3-n}^{2-}$ (Ch = Se or Te), Pb_2SSeTe^{2-}, and $M_2Se_3^{2-}$ (M = Sn and/or Pb). The $M_2Ch_3^{2-}$ anions all have compressed trigonal bipyramidal structures with the equatorial chalcogen atoms bonded to the axial group 14 metal atoms. The small Ch–M–Ch (90°) and M–Ch–M (70°) angles of the $M_2Ch_3^{2-}$ anions as well as their low relativistically corrected coupling constants, $^1K(M–Ch)_{RC}$, suggest substantial valence p-orbital involvement in the trigonal bipyramidal cage bonding. This is in accord with the previously suggested molecular bonding framework[2] which can be described as follows: two valence p orbitals of each chalcogen atom are directed toward the apical metal atoms while the third is tangential and nonbonding in the equatorial plane; all three valence p orbitals of the apical atoms lie along the edges of the MCh_3 moiety in the trigonal bipyramid.

The relatively short M···M distances in the trigonal bipyramidal $M_2Ch_3^{2-}$ anions are all significantly shorter than their van der Waals distances. However, it is not reasonable to use the sum of the van der Waals radii as estimates for the sizes of the apical atoms as they include contributions from the valence p orbitals. It is more appropriate to use the M^{2+} cores of the apical atoms ([Kr]4d^{10}5s^2, Sn and [Xe]5d^{10}6s^2, Pb) which can be estimated from the M^{2+} univalent radii.[35] The ionic radii of In^+ (1.32 Å) and Tl^+ (1.40 Å) provide an estimate for the upper limit of the univalent radii of Sn^{2+} and Pb^{2+}, respectively. Doubling of these upper limit radii gives Sn···Sn (2.64 Å) and Pb···Pb (2.80 Å) distances which are considerably shorter than those observed in the trigonal bipyramidal $M_2Ch_3^{2-}$ anions. Thus it appears that the short M···M distances could in turn be responsible for the relatively large spin-spin coupling constants observed between the apical atoms.

Short M···M distances have also been observed in related trigonal bipyramidal cage molecules.[36] In structurally closely related cases where axial Tl(I) or In(I) and Sn(II) atoms are bonded to three equatorial *t*-BuO ligands,[36a,b] the short Sn(II)···M distances may also be regarded as resulting from geometrical constraints imposed by the metal–oxygen bonding.

Experimental Section

Apparatus and Materials. The compounds reported here were all air sensitive. Consequently, all manipulations were carried out under rigorous anhydrous and oxygen-free conditions on glass vacuum lines equipped with glass/Teflon grease-free stopcocks (J. Young) or in a nitrogen-filled drybox (Vacuum Atmospheres Model DLX) as previously described.[2,3,5] Potassium (MCB) was used as received, and freshly cut samples were handled only in the drybox. Lead, as shot (British Drug House, 99.99%), tellurium powder (Alfa Inorganics, 99.5%), selenium powder (Alfa Inorganics, 99.9%), sulfur (BDH Chemicals), tin shot (Baker Analyzed, 99.9%), PbSe (Alfa Products, 99.99%), and 2,2,2-crypt (4,7,13,16,21,24-hexaoxa-1,10-diazabicyclo[8.8.8]hexacosane) (Merck, 99%, or Aldrich, 98%) were vacuum-dried but otherwise used as received. Potassium monoselenide, K_2Se, was prepared as described in ref 37. Ethylenediamine (Fisher Scientific Co.) was dried over CaH_2 (MCB) for several weeks and then vacuum-distilled onto and stored over fresh CaH_2 for at least a further week prior to use.

Preparation of Alloys. The K–Pb–Ch and K–Sn–S–Te alloys were prepared by fusion of the elements in approximately 1:1:1 and 1:1:0.33:0.67 ratios, respectively, in thick-walled glass tubes as described previously.[2,3,5] KPbS: K (5.737 g, 146.7 mmol), Pb (5.461 g, 26.36 mmol), S (5.480 g, 170.9 mmol). $KPbSe_{0.32}S_{0.63}$: K (12.60 g, 322.2 mmol), Pb (12.00 g, 57.92 mmol), Se (4.029 g, 51.02 mmol), S (7.994 g, 249.3 mmol). $KPbSe_{0.63}S_{0.32}$: K (6.860 g, 175.5 mmol), Pb (6.530 g, 31.52 mmol), Se (4.354 g, 55.14 mmol), S (2.177 g, 67.89 mmol). $KPbTe_{0.35}S_{0.64}$: K (7.993 g, 204.4 mmol), Pb (7.612 g, 36.74 mmol), Te (2.803 g, 21.97 mmol), S (5.131 g, 160.0 mmol). $KPbTe_{0.70}S_{0.32}$: K (12.22 g, 312.5 mol), Pb (11.65 g, 56.23 mmol), Te (8.572 g, 67.18 mmol), S (3.877 g, 120.9 mmol). $KPbTe_{0.35}Se_{0.32}S_{0.33}$: K (8.361 g, 213.8 mmol), Pb (7.965 g, 38.44 mmol), Te (2.927 g, 22.94 mmol), Se (2.657 g, 33.65 mmol), S (2.748 g, 85.70 mmol). $KSnS_{0.33}Te_{0.67}$: K (0.255 g, 6.52 mmol), Sn (0.776 g, 6.54 mmol), Te (0.5601 g, 4.39 mmol), S (0.0702 g, 2.19 mmol). The brittle alloys were ground and their compositions corrected for recovered malleable lead and tin lumps. The stoichiometries of the final alloys were $KPb_{0.40}S_{0.96}$, $KPb_{0.46}Se_{0.32}S_{0.63}$, $KPb_{0.45}Se_{0.63}S_{0.32}$, $KPb_{0.35}Te_{0.35}S_{0.64}$, $KPb_{0.50}Te_{0.70}S_{0.32}$, $KPb_{0.35}Te_{0.35}Se_{0.32}S_{0.33}$, and $KSn_{0.53}S_{0.33}Te_{0.67}$. The SnSe and SnTe alloys were prepared by fusion of the elements in quartz tubes using a natural gas/oxygen torch-flame.

Preparation of $Pb_2Ch_3^{2-}$ (Ch = S/Se, S/Te, S/Se/Te) Solutions. For the preparation of each anion series in solution, the appropriate K–Pb–Ch alloy powder was extracted in en in the presence of stoichiometric amounts of 2,2,2-crypt and the final solution was isolated for NMR spectroscopy as described previously:[2,3,5] $Pb_2S_3^{2-}$ ($KPb_{0.40}S_{0.96}$ 0.0773 g, 0.506 mmol; 2,2,2-crypt 0.1939 g, 0.515 mmol); $Pb_2S_kSe_{3-k}^{2-}$($KPb_{0.46}Se_{0.32}S_{0.63}$ 0.0616 g, 0.342 mmol; 2,2,2-crypt 0.1282 g, 0.340 mmol; $KPb_{0.45}Se_{0.63}S_{0.32}$ 0.0648 g, 0.320 mmol; 2,2,2-crypt 0.1277 g, 0.339 mmol); $Pb_2S_mTe_{3-m}^{2-}$ ($KPb_{0.35}Te_{0.35}S_{0.64}$ 0.0575 g, 0.325 mmol; 2,2,2-crypt 0.1250 g, 0.332 mmol; $KPb_{0.50}Te_{0.70}S_{0.32}$ 0.0927 g, 0.383 mmol; 2,2,2-crypt 0.1288 g, 0.342 mmol); $Pb_2S_nSe_{m-n}Te_{3-m-n}^{2-}$ ($KPb_{0.32}Te_{0.35}Se_{0.32}S_{0.33}$ 0.0512 g, 0.275 mmol; 2,2,2-crypt 0.1105 g, 0.293 mmol).

Preparation of $M_2Se_3^{2-}$ (M = Sn, Sn/Pb) Solutions. The procedures were similar to those used to extract K–Pb–Ch alloys and involved reactions of K_2Se with SnSe or SnSe/PbSe powders in ethylenediamine in the presence of 2,2,2-crypt. Extraction times were typically 4-10 weeks at room temperature before the solutions were isolated for NMR spectroscopy. In a typical preparation yielding the $Sn_2Se_3^{2-}$ and $SnPbSe_3^{2-}$ anions, the following amounts of reagents were used. $Sn_2Se_3^{2-}$: K_2Se (0.044 g, 0.28 mmol), SnSe (0.112 g, 0.567 mmol), 2,2,2-crypt (0.215 g, 0.570 mmol). $SnPbSe_3^{2-}$: K_2Se (0.113 g, 0.716 mmol), SnSe (0.071 g, 0.36 mmol), PbSe (0.307 g, 1.07 mmol), 2,2,2-crypt (0.569 g, 1.51 mmol).

Multinuclear Magnetic Resonance Spectroscopy. All ^{77}Se, ^{117}Sn, ^{119}Sn, ^{125}Te, and ^{207}Pb spectra were recorded on Bruker WM-250 and AM-500 (^{77}Se NMR of the $SnPbSe_3^{2-}$ solution only) pulse spectrometers. Spectra were routinely obtained without locking (field drift <0.1 Hz h^{-1}) using 10-mm probes broad-banded over the frequency ranges 12–101 MHz (5.8719 T) and 23–202 MHz (11.475 T), respectively. The observing frequencies were 95.383 MHz (^{77}Se) on the AM-500 spectrometer and 47.704 MHz (^{77}Se), 89.128 MHz (^{117}Sn), 93.276 MHz (^{119}Sn), 78.917 MHz (^{125}Te), and 52.174 MHz (^{207}Pb) on the WM-250 spectrometer. Free-induction decays were typically accumulated in 32K memories. Spectral width settings of 25–100 kHz were employed, yielding data point resolutions of 3.0–6.1 Hz and acquisition times of 0.328–0.655 s, respectively. A sample typically required 100 000–300 000 free induction decays. Pulse widths for the bulk magnetization tip angles of approximately 90° were 25–30 (^{77}Se), 40 (^{117}Sn), 25–28 (^{119}Sn), 25–30 (^{125}Te), and 25–33 μs (^{207}Pb) for the WM-250 spectrometer and 6–12 μs (^{77}Se) for the AM-500 spectrometer. Line-broadening parameters used in exponential multiplication of the free-induction decays were 5–20 Hz.

The respective nuclei were referenced to neat samples of $(CH_3)_2Se$, $(CH_3)_2Te$, $(CH_3)_4Sn$, and $(CH_3)_4Pb$ at 24 °C. The chemical shift convention used was a positive (negative) sign signifies a chemical shift to high (low) frequency of the reference compound.

Crystal Structure Determinations of (2,2,2-crypt-K^+)$_2Sn_2Te_3^{2-}$ and (2,2,2-crypt-K^+)$_2Sn_2Se_3^{2-}$. Crystal Growing. (2,2,2-crypt-K^+)$_2Sn_2Te_3^{2-}$.

(34) Cisar, A.; Corbett, J. D. *Inorg. Chem.* **1977**, *16*, 632.
(35) (a) Pauling, L. *The Nature of the Chemical Bond*, 3rd ed.; Cornell University Press: Ithaca, NY, 1960; Chapter 13, pp 511–519. (b) Kammeyer, C. W.; Whitman, D. R. *J. Chem. Phys.* **1972**, *56*, 4419.
(36) In Tl(*t*-BuO)$_3$Sn,[a] the Tl···Sn distance is 3.306(3) Å and $^2J(^{205,203}Tl–^{119}Sn)$ = 1293 Hz (van der Waals contact 4.2 Å),[3] while, in In(*t*-BuO)$_3$Sn,[b] the In···Sn distance is 3.200(3) Å (van der Waals contact 3.1 Å).[3] The distance between tin and thallium or indium is somewhat decreased in mono- or diadducts such as (CO)$_5$Mo–Sn(*t*-BuO)$_3$Tl [Sn···Tl = 3.298(1) Å][b] and (CO)$_5$Cr–In(*t*-BuO)$_3$Sn–Mo(CO)$_5$ [Sn···In = 3.087(2) Å].[b] In the structure of Bi$_2$[W(CO)$_5$]$_3$, there is a Bi_2W_3 moiety of D_{3h} symmetry in which the Bi···Bi distance of 2.815(7) Å is 0.26 Å shorter than that in Bi metal (3.071 Å).[c] (a) Veith, M.; Rösler, R. *Angew. Chem., Int. Ed. Engl.* **1982**, *21*, 858. (b) Veith, M.; Kunze, K. *Angew. Chem., Int. Ed. Engl.* **1991**, *30*, 95. (c) Huttner, G.; Weber, U.; Zsolnai, L. *Z. Naturforsch.* **1982**, *37B*, 707.

(a) The alloy $KSn_{0.53}S_{0.33}Te_{0.67}$ (96.8 mg, 0.438 mmol) was rapidly extracted in en and in the presence of 2,2,2-crypt (174.7 mg, 0.465 mmol) to produce a red-brown solution, the color of which changed to red-orange on standing for 1 week. Dark red crystals, suitable for X-ray diffraction, simultaneously appeared. After isolation, the crystals were transferred to a drybox equipped with a microscope. The crystals were dark red plates and were mounted and sealed in 0.2 mm Lindemann glass capillaries; X-ray data were recorded at −100 °C.

(b) The extraction of K_2Te with SnTe in a ratio 1:2 in liquid ammonia rapidly produced a red-orange solution which turned red-brown on the addition of 2,2,2-crypt. After several days, the solution turned red whereupon an orange precipitate and violet and red crystals appeared. The violet crystals were shown by a unit cell determination to be (2,2,2-crypt-$K^+)_2Te_4^{2-}$,[38] while the red crystals were (2,2,2-crypt-$K^+)_2$-$Sn_2Te_3^{2-}$. The red crystals were hexagonal plates and were mounted and sealed in 0.1-mm Lindemann glass capillaries; X-ray data were recorded at 24 °C.

(2,2,2-crypt-$K^+)_2Sn_2Se_3^{2-}$. The extraction of K_2Se (48.7 mg, 0.310 mmol) along with SnSe (119.2 mg, 0.603 mmol) in en in the presence of 2,2,2-crypt (237.2 mg, 0.629 mmol) gave a yellow-green solution which remained unchanged over a period of several weeks. ^{119}Sn and ^{77}Se NMR spectra were first obtained, and the solution was shown to contain mainly the $Sn_2Se_3^{2-}$ anion. The solution was then transferred to another reactor in a dry nitrogen atmosphere and slowly concentrated under dynamic vacuum. During the concentration process, crystallization started. After the concentrated sample was flame-sealed, a large number of yellow plates deposited on the walls of the reactor. The mother liquor was decanted, and the tube was cut open in an inert atmosphere so that the crystals adhering to the sample tube walls could be dried under dynamic vacuum. The dry sample was transferred to a drybox equipped with a microscope and the crystals were mounted and sealed in 0.2–0.3-mm Lindemann glass capillaries.

Collection and Reduction of X-ray Data. (2,2,2-crypt-$K^+)_2Sn_2Te_3^{2-}$. The collection and reduction of X-ray data as well as the refinement of the structure were carried out in similar fashions for both data sets. The experimental values at 24 °C are given in square brackets.

Preliminary oscillation and Weissenberg photographs revealed that the crystals were single; diffraction spots displayed $\bar{3}m$ trigonal symmetry. The best crystals were then centered on a Siemens P3 diffractometer. Accurate cell dimensions were determined at $T = -100$ °C [24 °C] from a least-squares refinement of the setting angles (χ, ϕ, 2θ) obtained from 15 [21] accurately centered reflections (with $18.33° \le 2\theta \le 20.99°$) chosen from a variety of points in reciprocal space. Integrated diffraction intensities were collected using the ω-scan technique, the slowest scan rate being 4°/min (in 2θ) so that the weaker reflections were examined most slowly to minimize counting errors. The data were collected with -15 [-11] $\le h \le 15$ [11], $0 \le k \le 15$ [11], and -25 [0] $\le l \le 25$ [21] and with 2 [3]° $\le 2\theta \le 45$ [30]°, using molybdenum [silver] radiation monochromatized with a graphite crystal ($\lambda = 0.710\,73$ [0.560 86] Å). During data collection, the intensities of three standard relections were monitored every 48 [97] reflections to check for crystal stability and alignment. A total of 7533 [2385] reflections were collected, no significant variations in the intensities of the standards were observed. A total of 1148 [739] unique reflections remained after averaging of equivalent reflections. A total of 757 [305] reflections, satisfying the condition $I \ge 2$ [2]$\sigma(I)$, were used for structure solution. These reflections exhibited systematic absences for $h\bar{h}0l$, $l = 2n$, and 0001, $l = 2n$. Corrections were made for Lorentz and polarization effects. Absorption corrections were applied by using the programs DIFABS and Texsan[39] for the data set at −100 °C, while the ϕ-scan method ($\Delta\phi = 10°$) was used for the data set at 24 °C ($\mu\bar{R} = 2.09$ cm^{-1}).

(2,2,2-crypt-$K^+)_2Sn_2Se_3^{2-}$. The crystal was centered on a Siemens P4 diffractometer equipped with a rotating anode. Accurate cell dimensions were determined at 24 °C from a least-squares refinement of the setting angles (χ, ϕ, 2θ) obtained from 29 accurately centered reflections (with $10.19° \le 2\theta \le 25.00°$) chosen from a variety of points in reciprocal space. Their peak profiles revealed that the crystal was single. Integrated diffraction intensities were collected using an ω-scan technique (slowest rate 1.5°/min) with $-1 \le h \le 11$, $-1 \le k \le 49$, and $-12 \le l \le 12$ and with $3° \le 2\theta \le 45°$, using molybdenum radiation monochromatized with a graphite crystal ($\lambda = 0.710\,73$ Å). During data collection, the intensities of three standard reflections were monitored every 97 reflections to check for crystal stability and alignment; some decay was observed (20%) and was corrected. A total of 9073 reflections were collected, and these exhibited extinctions for $h0l$, $I \ne 2n$, $0k0$, $k \ne 2n$ and $00l$, $l \ne 2n$; the monoclinic space group $P2_1/n$ (No. 14) proved to be the only space group having the appropriate extinction conditions. A total of 7240 unique reflections remained after averaging of equivalent reflections, and a total of 3016 reflections were "observed" by the criterion $I > 2\sigma(I)$. Corrections were made for Lorentz and polarization effects, and absorption corrections were applied by using the programs DIFABS and Texsan.[39]

Crystal Data. (2,2,2-crypt-$K^+)_2Sn_2Te_3^{2-}$: $C_{36}H_{72}K_2N_4O_{12}Sn_2Te_3$ (fw = 1451), trigonal, space group $P\bar{3}c1$, (a) (at −100 °C) $a = 11.703(4)$ Å, $c = 21.945(6)$ Å, $V = 2603$ Å^3, and $D_{calc} = 1.852$ g cm^{-3} for $Z = 2$, Mo Kα radiation ($\lambda = 0.710\,69$ Å, μ(Mo Kα) = 28.2 cm^{-1}); (b) (at 24 °C) $a = 11.817(9)$ Å, $c = 22.01(2)$ Å, $V = 2662$ Å^3, and $D_{calc} = 1.811$ g cm^{-3} for $Z = 2$, Ag Kα radiation ($\lambda = 0.560\,86$ Å, μ(Ag Kα) = 14.6 cm^{-1}).

(2,2,2-crypt-$K^+)_2Sn_2Se_3^{2-}$: $C_{36}H_{72}K_2N_4O_{12}Sn_2Se_3$, fw = 1305.44), monoclinic, space group $P2_1/n$, with $a = 10.342(3)$ Å, $b = 46.976(6)$ Å, $c = 11.402(4)$ Å, $\beta = 90.15(3)°$, $V = 5539(3)$ Å^3, and $D_{calcd} = 1.565$ g cm^{-3} for $Z = 4$, Mo Kα radiation ($\lambda = 0.710\,73$ Å, μ(Mo Kα) = 30.7 cm^{-1}).

Solution and Refinement of the Structures. (2,2,2-crypt-$K^+)_2Sn_2Te_3^{2-}$. The XPREP program[40] was used for determining the correct cell and space group. The original cell was first confirmed, showing the lattice to be trigonal primitive ($R_{int} = 0.034$ [0.041]). The two space groups that were consistent with the systematic absences (n-glide and C_3) were the centrosymmetric $P\bar{3}c1$ and the noncentrosymmetric $P3c1$ space groups. The structure was shown to be centrosymmetric by an examination of the E statistics (calculated 0.952 [0.852]; theoretical 0.968), and consequently the structures were solved in the $P\bar{3}c1$ (No. 165) space group.

For both compounds, solutions were obtained (at −100 °C, a first solution was obtained without absorption correction) by conventional direct methods which located the positions of the tin and potassium atoms on special positions (i.e., 3..(c), 3..(d)) for both data sets while the tellurium atoms were found to occupy general positions at −100 °C and special positions (i.e., 3..(c)) at 24 °C. The model at −100 °C implied a disorder in the "equatorial" plane of the anion, and consequently the site occupancy factors of the tellurium atoms were set equal to 0.50 instead of 1.00. The full-matrix least-squares refinement of the positions and isotropic thermal parameters of all atoms gave a conventional agreement index R ($=\sum||F_o| - |F_c||/\sum|F_o|$) of 0.45 [0.35]. Successive difference Fourier syntheses revealed the positions of all the remaining N, O, and C atoms. The nitrogen atoms were located on special positions (i.e., 3..(d)) and the carbon and oxygen atoms on general positions. A significant improvement of the structure was achieved by introducing the positions and isotropic thermal parameters for the N, O, and C atoms. The R factor dropped to 0.175 [0.22]. The introduction of anisotropic thermal parameters for the Sn, Te, and K atoms produced another important improvement of the structure ($R = 0.093$ [0.103]). Finally, a slight change in the R factor ($R = 0.076$ [0.098]) was obtained by introducing anisotropic [isotropic] thermal parameters for the N, O, and C atoms and calculated values of the positions of the hydrogen atoms (d(C–H) = 0.96 Å; U(H) fixed to 0.08 Å^2); $R = 0.074$ [0.098]. The introduction of a weighting factor ($w = 1/\sigma^2(F) + 0.0017F^2$) gave a final solution with $R = 0.107$ ($R_w = 0.080$) for the data set at 24 °C.

The structure of the first data set was solved a second time using data that had been corrected for absorption. The initial model used the atomic coordinates and isotropic thermal parameters defined previously for the Sn, Te, K, N, O, C, and H atoms. The solution obtained ($R = 0.118$) indicated a significant improvement over that obtained without absorption corrections ($R = 0.169$). The structure was improved by introducing anisotropic thermal parameters for the Sn, Te, and K atoms ($R = 0.066$). The N, C, and O atoms could also be refined with anisotropic thermal parameters ($R = 0.062$). The final refinement was obtained by introducing a weighting factor ($w = = 1/\sigma^2(F) + 0.00046F^2$) and gave rise to a residual, R, of 0.063 ($R_w = 0.071$).

(2,2,2-crypt-$K^+)_2Sn_2Se_3^{2-}$. The XPREP program[40] was used for determining the correct cell and space group and first confirmed the original cell and that the lattice was monoclinic primitive ($R_{int} = 0.024$). The structure was shown to be centrosymmetric by an examination of the E statistics (calculated 1.018; theoretical 0.968). As mentioned before, the only space group that proved to be consistent with the systematic extinction conditions was the centrosymmetric space group $P2_1/n$; consequently, the structure was solved in that space group.

(37) Björgvinsson, M.; Schrobilgen, G. J. *Inorg. Chem.* **1991**, *30*, 2540.
(38) Devereux, L. A.; Schrobilgen, G. J.; Sawyer, J. F. *Acta Crystallogr.* **1985**, *C41*, 1730.
(39) Walker, N.; Stuart, D. *Acta Crystallogr.* **1983**, *A39*, 158.

A first solution was obtained without absorption corrections, and it was achieved by direct methods, which surprisingly located the general positions of all the atoms of the anion and both cations of the asymmetric unit. Interestingly, as previously observed for $Pb_2Se_3^{2-}$,[2] the peak height for one Se atom appeared to be much less than those for the other two Se atoms and resulted in a higher temperature factor in the least-squares refinement. The full-matrix least-squares refinement of the atom positions and isotropic thermal parameters gave a conventional R ($=\sum||F_o| - |F_c||/\sum|F_o|$) of 0.18. The resulting difference Fourier synthesis revealed the general positions of all the remaining carbon atoms. The introduction of the positions and isotropic thermal parameters for all the Sn, Se, K, N, O, and C atoms as well as the calculated values of the positions of the hydrogen atoms [d(C–H) = 0.96 Å; U(H) fixed to 0.08 Å^2] resulted in a drop of the R factor to 0.164. The tin, selenium, and potassium atoms were ultimately refined with anisotropic thermal parameters, while light atoms in the ligands were restricted to isotropic thermal parameters, producing another significant improvement of the structure (R = 0.084).

The structure was solved a second time using data that had been corrected for absorption. The initial model used the atomic coordinates and isotropic thermal parameters defined previously for the Sn, Se, K, N, O, C, and H atoms. The solution obtained (R = 0.139) indicated some improvement over that obtained without absorption corrections (R = 0.164). The final refinement was obtained by introducing anisotropic thermal parameters for the Sn, Se, and K atoms and by setting the weight factor equal to zero, giving rise to a residual, R, of 0.0899 (R_w = 0.0777). In the final difference Fourier map, the maximum and the minimum electron densities were 1.35 and –1.33 e Å^{-3}.

All calculations were performed on a 486 personal computer, using the SHELXTL PLUS™ (Sheldrick, 1990)[40] determination package for structure solution and refinement as well as structure determination molecular graphics.

Acknowledgment. We thank the Natural Sciences and Engineering Research Council of Canada for support in the form of an operating grant; the Ministry of Foreign Affairs, France, for the award of a Lavoisier Fellowship to H.P.A.M.; McMaster University and the Ontario Ministry of Colleges and Universities for the award of scholarships to M.B.; and the German Academic Exchange Service (DAAD) for the award of a travel grant to G.S.

Supplementary Material Available: Tables VII–X, giving structure determination parameters, anisotropic thermal parameters, the remaining distances and angles in the 2,2,2-crypt-K$^+$ cations, and atomic coordinates for the hydrogen atoms, and Figures 7–9, showing stereoviews of the unit cell of 2,2,2-crypt-K$^+$ ([001], –100 °C; [001], 24 °C; [100], 24 °C) (15 pages). Ordering information is given on any current masthead page. Tabulations of the observed and calculated structure factors (Tables XI–XIII) are available upon request from G.J.S. up to 1 year from the date of publication.

(40) Sheldrick, G. M. *SHELXTL PLUS*, Release 4.21/V; Siemens Analytical X-Ray Instruments, Inc.: Madison, WI, 1990.